Escola d'Enginyeria de Telecomunicació i Aeroespacial de Castelldefels

UNIVERSITAT POLITÈCNICA DE CATALUNYA

TREBALL FINAL DE GRAU

TÍTOL DEL TFG: PARAMETRIC UAS LEG DESIGN FOR ATMOSPHERIC STRUCTURE INVESTIGATION

TITULACIÓ: Grau en Enginyeria d'Aeronavegació

AUTOR: Antoni Mora Cidoncha

DIRECTOR: Enric Pastor Llorens

DATA: 22 de maig del 2015

Títol: Parametric UAS leg design for atmospheric structure investigation

Autor: Antoni Mora Cidoncha

Director: Enric Pastor Llorens

Data: 22 de maig del 2015

Resum

Els tornados són un dels fenòmens atmosfèrics més devastadors que existeixen al món. Només als Estats Units, de mitjana, hi ha 1400 tornados anuals. Tot i la repercussió i els esforços per poder predir el moviment i la força d'aquests, el cert és que no hi ha un model que predigui la posició dels tornados a més de 30 minuts vista. Des de fa 50 anys, hi ha la certesa que una part concreta dels tornados, el Rear-Flank Downdraft (RFDs), és clau en la formació i intensificació de tornados. Aquesta zona ha estat molt documentada aquests anys, però el seu rol dinàmic encara no està documentat. Recentment, hi ha hagut experiments on s'han enviat avions RC no tripulats (UAs) a investigar aquestes zones dels tornados.

El grup de recerca Icarus ha desenvolupat un UAS (Unmanned Aircraft System) definit per diversos serveis que cooperen per fer que el FMS (Flight Managment System) pugui volar fent servir guiatge per waypoints. El sistema i les missions han estat implementats basats en paràmetres reconfigurables que permeten fer *scans* dinàmics paramètrics. És a dir, que poden descriure totes les trajectòries necessàries per fer una missió amb la definició de certs paràmetres.

L'objectiu d'aquest treball de final de grau ha sigut, aprofitant les possibilitats que els *scans* paramètrics del UAS del grup de recerca Icarus ens ofereixen, dissenyar un nou tipus de *scans* per la recerca dels RFD. De tal manera que els UAS volin d'una manera més intel·ligent a través d'aquesta part dels tornados amb l'objectiu de poder fer els màxims *samples* possibles, per la recollida de dades, tenint en compte les característiques tant dels RFDs com per a aplicacions atmosfèriques més genèriques.

A partir d'unes hipòtesis sobre les necessitats d'aquets tipus de *scans*, s'ha procedit a desenvolupar el Curved Scan. S'han discutit la definició de paràmetres i el refinament d'aquests per tal de fer un algorisme robust. També, degut a la importància de la rapidesa de les missions, del tipus de traces i de com s'enllacen, s'ha desenvolupat un nou tipus de gir -amb una extensió per altres possibles aplicacions-. Finalment, s'ha implementat dins de l'entorn de simulació, amb exemples concrets, i s'ha vist la possible aplicació d'aquest nou tipus de *scans* en el *surveillance* amb UAS dels núvols de cendra que expulsen els volcans.

Title: Parametric UAS leg design for atmospheric structure investigation

Author: Antoni Mora Cidoncha

Director: Enric Pastor Llorens

Date: May 22 nd 2015

Overview

Tornadoes are one of the most devastating atmospheric phenomena worldwide. Only in the EEUU, there are more than 1400 tornadoes yearly. Despite the great effort trying to understand and predict the behavior and path of the tornadoes, the truth is that there not exists an accurate model yet. For more than 50 years, it has been summarized the importance of a certain zone of the tornadoes, the Rear-Flank Downdraft (RFD), on tornado genesis and intensification. This zone is well documented, but its dynamic role it is not understood yet. Recently, some experiments has sent RC Unmanned Aircraft (UA) to sample this zone.

The research group Icarus has developed an UAS (Unmanned Aircraft System) defined by a sort of services which cooperate together so as the FMS (Flight Management System) being able to fly using a basic waypoint guidance. The whole system and missions have been developed by using reconfigurable parameters that allow dynamic parametrical scans. That is, instead of specifying the complete trajectory of the mission, it is just need to define some parameters.

The motivation of this final project degree has been, taking advantage of the possibilities of the parametrical scans of the Icarus research group UAS bring us, to design a new scan type to do a research on RFD environment. This way, enabling the UAS to fly wisely through this part of the tornadoes with the goal of developing a sample strategy to collect the maximum possible in situ data, regarding both the RFD characteristics as well as possible more generic atmospheric applications.

Starting from some hypothesis about the needs on this new kind of scans, the Curved Scan has been developed. There has been a parameter discussion and its refinements so as to obtain a robust algorithm. In addition, due to the importance of the quickness of this missions, the sort of traces and how they are linked to each other, a new turn type has been developed -as well as an extension for further applications-. Finally, it has been implemented inside the simulation environment, with particular examples, and it has been shown the applicability of this new scan type in the surveillance with UAS of the volcanic plumes.

ÍNDEX

INTRODUCTION

The goal of this project is to design a new scan type, on a parametric scan context, for Unmanned Aircraft Systems (UAS) in order to improve atmospheric research. This will be accomplished by understanding the theory behind of the atmospheric phenomena and its physics so as to make out the needs of this sort of mission, as well as, having a deep comprehension of what parametric scan allows to do. This project will be divided into three mainly different parts; the first one, where it is introduced both the theoretical aspects related to the atmospheric phenomena and the developing environment. The second one, where it is fully explained how the algorithm has been developed and implemented and how it works. And a third one, where particular examples will be exposed so as to show the accomplishment of the proposed task.

In the first chapter we can find an introduction into the problematic of tornadoes all over the EEUU and the actual state of art of tornadoes research. There exists an overview of the importance of a certain zone of tornadoes, the Rear-Flank Downdraft (RFD), which has been demonstrated to be critical in the genesis and intensification of tornadic storms. Then, it is exposed a summary of the actual atmospheric research with UAS. Finally, it can be found a brief of the simulation environment of the Icarus research group. Here, it will be summarized the actual parametric scan type of the group, its properties and characteristics.

In the second chapter we can see the steps followed to develop the new algorithm for the atmospheric research scan, in this case, to do the research on RFD. First of all, the algorithm developing needs of the scan are exposed referred to the actual parametric scan type. Then, it is explained how the properties of this zone will be interpreted as well as which will be the control variables for the user so as to have the desired scan path. Furthermore, a mathematical explanation of the developed new turn type is exposed. Finally, we can find a exhaustive explanation of each property of this new scan type and a summary of how the algorithm works depending on the user inputs.

In the third chapter we find the results of the implementation of this new algorithm in some particular cases, that is, how the new scan pattern looks like in real applications. It is also shown how changing the control variables -parameters of the scan- we are able to adapt the mission into the user behalf.

Finally, in the fourth chapter is briefly summarized other applications of this new scan type as well as the implementation of this new turn.

CHAPTER 1. GENERAL OVERVIEW

2.1 Physic problem explanation

The U.S. has sustained 170 weather/climate disasters since 1980 where overall damages/costs reached or exceeded $1 billion (including CPI adjustment to 2013). The total cost of these 170 events has exceeded $1 trillion [1].

In 2013, there were 9 weather/climate disaster events with losses exceeding $1 billion each across the United States [1]. These events included a drought event, 2 flooding events, and 6 severe storm events. Altogether, these events resulted in 113 deaths and had significant economic effects on the areas of impact [2].

Although tornadoes occur in many parts of the world, they are found most frequently in the United States. In an average year, 1,200 tornadoes cause 60-65 fatalities and 1,500 injuries and costs $400 million in damage nationwide. They take place mainly in central-north America like Texas, Kansas, Oklahoma, Nebraska or Missouri [3].

How do tornados form? Classically the answer has been "warm moist Gulf air meets cold Canadian air and dry air from the Rockies" however that is a gross oversimplification because, as National Oceanic and Atmospheric Administration state, the most thunderstorms that form under those conditions (near warm fronts, cold fronts and dry lines respectively) never make tornadoes. Even when the large-scale environment is extremely favorable for tornadic thunderstorms, not every thunderstorm spawns a tornado. The truth is that a accurately prediction model of tornadoes it is not found yet.

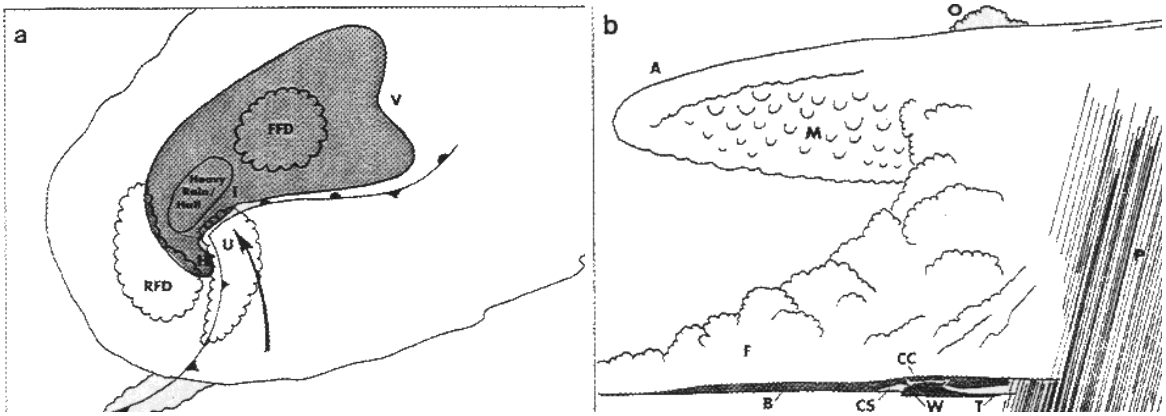

Figure 7.
Supercell. Schematic view of a classic supercell (a), and visual characteristics of the same storm as might be seen from the east or southeast (b). In (a), the region of radar reflectivity is shaded; note V-notch (V), inflow notch (I), and hook echo (H). Scalloped lines enclose region of main updraft (U), forward flank downdraft (FFD) and rear flank downdraft (RFD). Surface inflow is indicated by arrow. Frontal symbols indicate location of gust front. Features in (b) include overshooting top (O), backsheared anvil (A), mammatus (M), flanking line (F), rain-free base (B), clear slot (CS), collar cloud (CC), wall cloud (W), tail cloud (T) and area of heavy precipitation (P). Compare with Figs. 3 and 5.

Fig. 2.1 Schematic description of a general Supercell and its parts. Source: Southern Region Headquarters, National Oceanic and Atmospheric Administration: http://www.srh.noaa.gov/oun/?n=spotterglossary-figure7

Perhaps the best-recognized radar feature in a horizontal depiction associated with supercells[1] thunderstorms is the extension of low-level echo on the right-rear flank of these storms, called the ‘‘hook echo". According to Forbes (1981), "the hook represents a band of precipitation accompanied by downdraft and outflow, surrounding a weak echo region (a region of inflow and updraft)". Hook echoes are known to be associated with a commonly observed region of subsiding air in supercells, called the ‘‘rear-flank downdraft’’. It is usually placed at the western part of a tornado, far from the hail and strong winds and its shape is curved. It is usually delimited by the gust front. Most tornadoes develop coincident with the formation or intensification of the rear-flank downdraft.

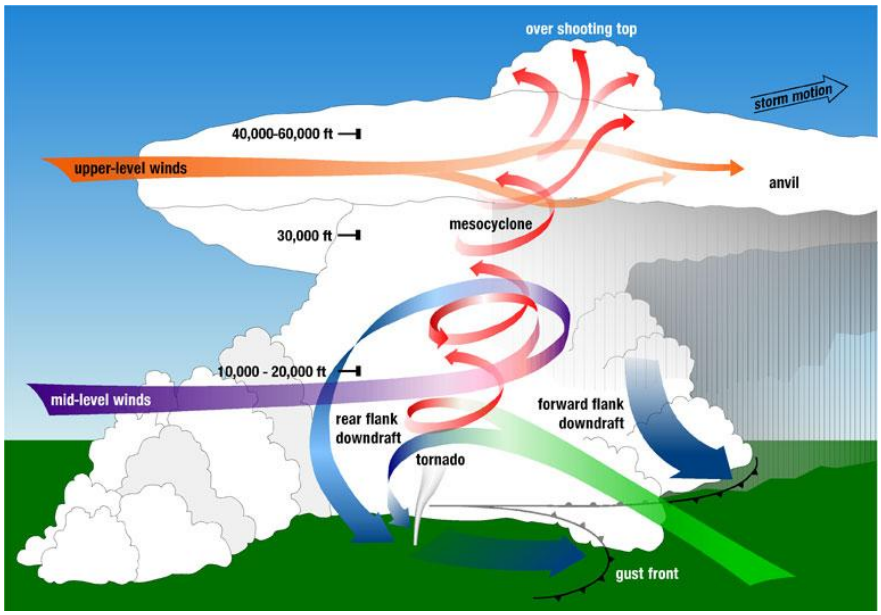

Fig. 2.2 "Tornadic supercell" by NOAA National Severe Storms Laboratory - http://www.nssl.noaa.gov/primer/tornado/images/tor_formation_lg.jpg.

[1] Supercells are storms - usually, but not necessarily, thunderstorms - with a well defined radar circulation called mesocyclone, that contains updrafts that rotate about a vertical axis. Supercells often produce damaging wind, large hail, and tornadoes, and most strong to violent tornadoes are associated with supercells.

Rear-flank downdrafts have been long surmised to be critical in the genesis of significant tornadoes[2] within supercell thunderstorms [4]. Some researches however, demonstrate that, sadly, hook echoes associated with tornadic and nontornadic supercell storms are indistinguishable in the radar(e.g., Trapp 1999, Wakimoto and Cai 2001), thus, we cannot be sure whether a storm could develop into a tornado or not by simply regarding the echoes.

Rear-flank downdrafts (RFDs) are regions of cold subsiding air that develop on the rear side of the main updraft of supercell storms. Visually are quite easy to see because they are manifested as a clear slot on the western side of a storm. The clearing comes as a result of rapidly sinking, warming air, which evaporates cloud droplets and rain drops, which creates the clear slot. The first experiment in this field with a RC plane that collected in-situ RFD measurements of wind-speeds showed that, even it was hard for the plane to keep the altitude, the mean values in that zones (at an average altitude of 1900m) were 20-30 m/s [5].

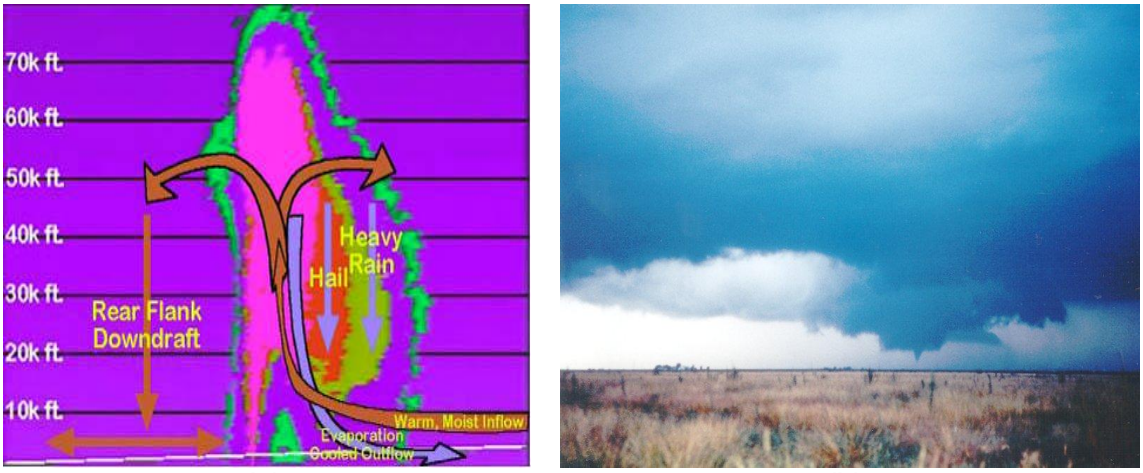

(a) (b)

Fig. 2.3 (a) Height and airflows inside a tornado (b) Manifestation of the RFD as a clear slot in the western part of a storm

Rear-flank downdrafts have been long thought (more than 50 years) to play an important role in tornadogenesis within supercell thunderstorms. However, its dynamical role in tornadogenesis is still not understood, despite a well-documented association between RFDs and its associated echo and tornado formation (e.g., Stout and Huff 1953; Ludlam 1963; Fujita 1975; Burgess et al. 1977).

The potential importance of the RFD in the genesis of the tornadoes also is suggested by observations that air entering the tornado or incipient tornado pass through the hook echo and RFD (Brandes 1978; Klemp et al. 1981; Dowell

[2] Not all supercells with RFD's produce tornadoes.

and Bluestein 1997). For example, visual observations by Brandes (1978), Lemon and Doswell (1979), Rasmussen et al. (1982), and Jensen et al. (1983) have shown or implied a near-total occlusion of the lowlevel mesocyclone[3] by the RFD prior to tornadogenesis. Furthermore, Wicker and Wilhelmson (1995) found that trajectories entering their simulated tornado-like vortex passed through the hook echo and RFD. So, depending on the properties of the RFD, for example if it is warm (because of its higher buoyancy), it can be incorporated into the rotating updraft, thus increasing rotation and the possibility of a tornado develop.

So, given the prior emphasis on the RFD in the tornadogenesis process and regarding the fact that RFD air parcels are thought to enter the tornado, the buoyancy and buoyancy gradients as well as thermodynamic properties in hook echoes and RFDs becomes to be highly important in the development, intensification, maintenance and diminution of near-surface rotation.

Very recent studies, that took part after the ending of the VORTEX[4] experiment, have shown, however, that even some special thermodynamic scenarios are critical for tornadogenesis, they are not sufficient to generate a tornado; another factors take part [6] [7]. In fact, some of its conclusions are "tornado likelihood, intensity, and longevity increase as the surface buoyancy, potential buoyancy (CAPE), and equivalent potential temperature in the RFD increase, and as the CIN associated with RFD parcels at the surface decreases.[..]While relatively warm, moist, and potentially buoyant RFD air parcels appear to be necessary for the genesis of significant tornadoes, this condition is not sufficient for tornadogenesis. Additional factors are almost certainly important (e.g., surface roughness and the angular momentum distribution through which the RFD descends)".

Regardless, as Markowsky [4] postuled, "If the hook echo and its associated RFD truly are critical to tornadogenesis, as hypothesized for many years, then perhaps significant gains in understanding will not be possible until more spatially and temporally detailed observations of this region can be made...", a necessity to collect data in and around the RFD exists so as to obtain better models for tornadogensis[5] and storms behaviour. This will be one of the main goals of VORTEX 2 experiment [7].

[3] A storm-scale region of rotation, typically around 2-6 miles in diameter and often found in the right rear flank of a supercell.

[4] J. M. Straka, R. P. Davies-Jones, C. A. Doswell, F. H. Carr, M. D. Eilts, and D. R. MacGorman, 1994: Verification of the Origins of Rotation in Tornadoes Experiment: VORTEX

[5] For a further understanding of what tornadogenesis is thought to imply, Tornadogenesis: Our current understanding, forecasting considerations, and questions to guide future research. Markowski, P. M., and Y. P. Richardson, 2009

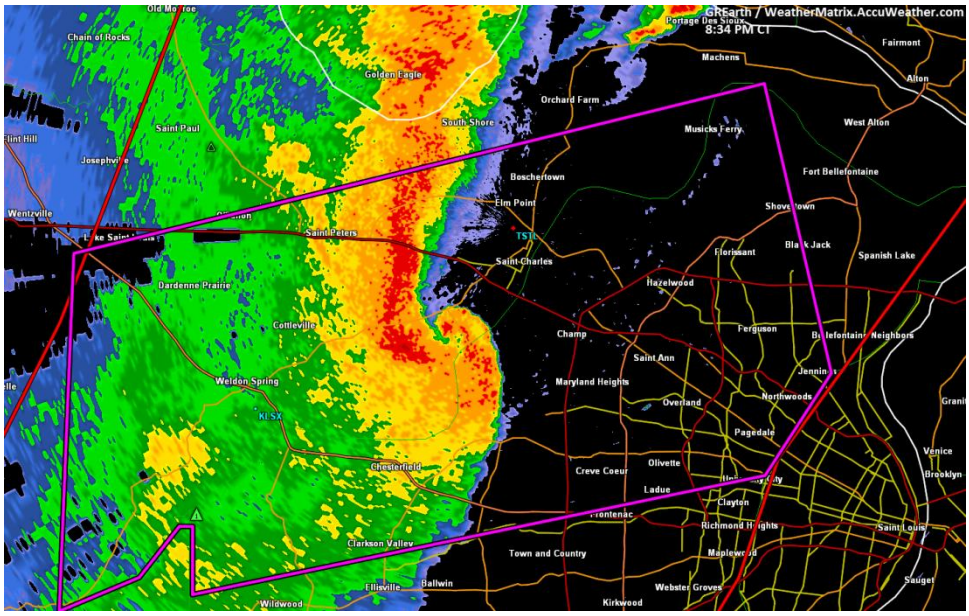

Fig. 2.4 Possible tornado intensification radar image over San Luis, Missouri. Clear distinction of the "hook echo" and the shaped form of the RFD

A possible solution to get data from RFDs may be using probes on the ground, but thermodynamic fields and their gradients cannot be ascertained above the surface by direct means. At best, only the sign of the gradients can be inferred above the surface, based on assumptions of the lapse rates beneath and at a distance from the storm [6]. Another solution could be using Doppler radars. However, they only can return detailed precipitation and wind-field data, but they cannot return directly-measured thermodynamic data, and manned aircraft involves too dangerous situations.

Therefore, Unmanned Aircraft Systems (UAS) seems to be the solution to the problem. Any human life compromised, relative low-cost solution and capable to get the airspeed needed to collect in situ data measurements of the thermodynamic characteristics of the atmosphere on the RFD and surroundings prior to a possible tornado.

Recently, researchers at the University of Colorado and University of Nebraska have collaborated to create a UAS (Tempest UA) for in situ interceptions and atmospheric sampling over severe storms [8]. Moreover, other investigators have developed a system based on hardware-in-loop to simulate UAS through severe storms combining a full six degree-of-freedom aircraft dynamic model with wind and precipitation data from simulated and actual severe convective storms [5]. However, neither of them have yet implemented any kind of scan model or sampling strategies for Unmanned Aircrafts (UA) in that environments, in which quickness of the mission and the samplings done is a tradeoff.

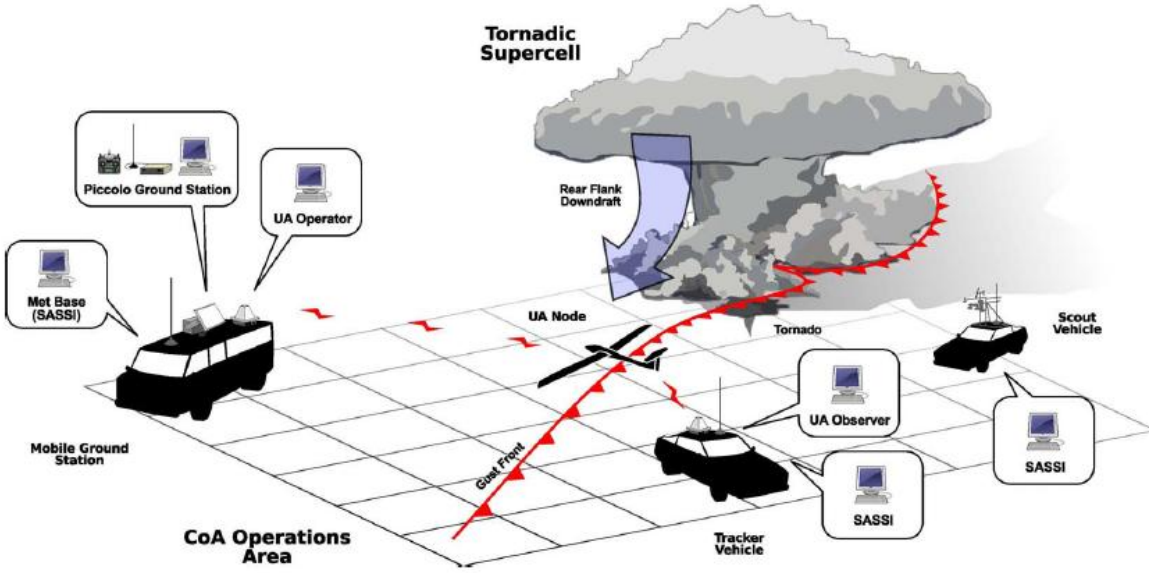

Fig. 2.5 Tempest UAS mission description on collaboration with VORTEX 2 experiment

Regarding the importance of the RFD areas within supercell thunderstorms and the actual research on that issue, the motivation of this project will be implementing a new type of scan pattern, on a parametric scan context, for UAS that will enable the aircraft to fly wisely trough a RFD in a remote sensing mission. The aircraft would carry with it some kind of thermodynamic sensors that would enable scientist collect data in that part of the supercell. This way, a possible experimental model for tornado develop or a possible prediction of its future behavior and intensity could be achieved, saving both human life and resources.

2.2 UAS in atmospheric environments

Unmanned aircraft have been used primarily for military applications. Today, unmanned (or more appropriately termed, *unoccupied)* aerial systems fly missions over agriculture fields so that farmers can monitor crop growth, aid topographic missions, help on fighting against fires, inspecting power lines, helping on border patrol missions and, obviously, in more commercial applications like picture filmmaking.

UAS are ideally suited for what engineers and practitioners call “3-D” missions, or those that are “dull, dirty, and/or dangerous". Today, as we are aware, there exists a wide spectrum of utilities. In this project, we are focusing on how UAS could help on atmospheric research. Nowadays, UAS are plenty used in that field, and many examples could be found.

EEUU, the largest investor in UAS technology worldwide, has developed many unmanned aircraft systems in atmospheric research. Hurricanes and tropical storms, as well as tornadoes, are one of the most destructive phenomena that Americans suffer. So, the study of them risking human life is too much dangerous. That is why UAS are perfect suited for that missions, because having a transmitter, which during these phenomena beam back measurements to scientists and operators safely on firm ground hundreds of miles away, mitigates any chance of danger to people involved in storm research. And with real-time transmission of data, even if the craft goes down, researchers will have all the measurements until the crash. One of the most used aircraft, before the development of better platforms, was the Orion and the G-IV jet hurricane hunters to observe the core of these storms.

Even the explosion of UAS use for commercial applications comes from (aprox) 5 years ago, NASA, by the late 1980s was already working on UAs, and on 2004, has terminated the Environmental Research Aircraft and Sensor Technology (ERAST) high altitude long endurance program. ERAST demonstrated the feasibility of constructing slow-flying UASs, capable of carrying sensors for scientific research, and capable of climbing to high altitudes. One of the achievements was the Helios UA, which was a solar powered UA that got to 96,863 feet on August 13th 2001 [9].

Nowadays, one of the most well-known HALE (high altitude large endurance) unmanned aircrafts of NASA are the Global Hawk and the Predator B Ikhana (the civil one). Global Hawk is the most common UAS used for hurricane and tropical storms overfly. NASA has developed two primarily missions in terms of study of hurricanes and tropical storms using the Global Hawk:

-HS3 Hurricane and Severe Storm Sentinel [10] is a five-year mission specifically targeted to investigate the processes that underlie hurricane formation and intensity change in the Atlantic Ocean basin. HS3 is motivated by hypotheses related to the relative roles of the large-scale environment and storm-scale internal processes. This mission has finalized the last 2014.

- The Genesis and Rapid Intensification Processes (GRIP) [11] experiment is a NASA Earth science field experiment in 2010 that will be conducted to better understand how tropical storms form and develop into major

hurricanes. This campaign will be conducted to capitalize on a number of ground networks, airborne science platforms, and space-based assets. The field campaign will be executed according to a prioritized set of scientific objectives.

However, HALE's are not the only UAS capable of atmospheric research. Aerosonde, Global Observer and Zephyr are other smaller UAs that are used in that field in other applications. In addition, most of Universities, not only in the States, have developed their own UAS. For example, the university of Bergen has developed the SUMO (Small Unmanned Meteorological Observer) to do a boundary layer research, or the university of Bristol, which has develop a light octocopter that can get to 9000 ft so as to sample greenhouse gases in the remote South Atlantic Ocean.

2.3 Parametric scan introduction

The research group Icaurs has developed a Unmanned Aircraft System, defined by a several services that work together and that enable the Flight Management System (FMS) of the Unmanned Aricraft Vehicle to fly using basic waypoint-based guidance. The main goal of the group is to take advantage of the UAs characteristics for civil applications.

Nowadays, a large market in civil applications is emerging around UAs. Regarding its characteristics, surveillance, may become its leading advantage [12]. Depending on the needs, flexibility during that kind of missions may be highly required due to their long endurance and ceiling, which may expose them to dangerous situations or putting them in conflict with ATC regulations and civil aviation. Therefore, a dynamic upgradable flight plans and its automatic execution is need to be performed to overcome those situations. However, in this moments, surveillance missions and its flight plans are pre-planned in advance and allow no re-planning once the flight take-off.

The Icarus UAS has been implemented by a flight plan specification language that provides re-configurable high-level constructs, which enable UAS flights to be adapted to the circumstances encountered during a mission [13]. In other words, the Icarus UAS surveillance missions are based on a parametrical, re-configurable structure, thus allowing a dynamical parametric scan (in a RNAV[6]-like context [14]).

Parametric legs[7], whose trajectory is computed by the FMS given a set of high-level, mission-oriented, dynamically upgradable parameters, are defined, together with the desired scanning area, to describe the sequence of waypoints that will determine the scan shape during a mission [15]. That is, given some

[6] RNAV is a method of navigation that permits aircraft operation on any desired flight path within the coverage of ground or space based navigation aids or within the limits of the capability of self-contained aids, or a combination of these.Source: Federal Aviation Administration

[7] A leg, the main flight plan component in RNAV, is described as the desired path, proceeding, following or between waypoints on a RNAV procedure.

set of data that the user has as a input and the desirable scanning area, approximating it as a closed polygon that tightly fits the exterior of its perimeter, the system is able to compute a sequence of tracks that, then, can be transformed into a sequence of flyable waypoints easily managed by the autopilot.

So, if the goal of the mission is exploring a given area, instead of specifying the complete trajectory, defining all scanning legs, we can provide the parameters that determine the geometry of the area (e.g. defining the polygon with clicks) and all of the legs necessary for its exploration will be automatically generated. This way, we can easily re-update in real time the exploration area just by updating a subset of those parameters.

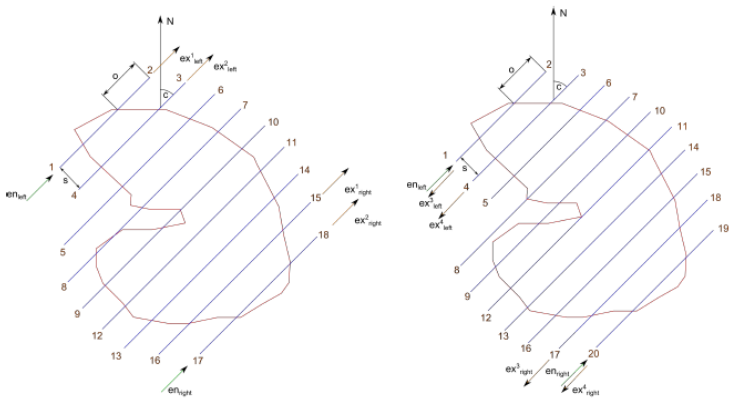

Fig. 2.6 Actual scanning like path for a parametrical missions

```
leg id="missionleg" xsi:type="BasicScanLeg">
  <course>45</course>
  <speed>150</speed>
  <altitude>4500</altitude>
  <trackseparation>1000</trackseparation>
  <exitcourse>False</exitcourse>
  <entryside>Left</entryside>
  <exitside>Left</exitside>
  <offset>5</offset>
  <entryoffset>10</entryoffset>
  <exitoffset>10</exitoffset>
  <initrack>1</initrack>
  <area>
    <point>41.9984726 1.9125963</point>
    <point>41.9002422 2.2004379</point>
    <point>41.8329421 2.5259285</point>
      <!-- More points may follow -->
  </area>
/leg>
```

Fig. 2.7 Set of parameters which defines any scanning mission

An example of the set of parameters and the scanning area it is shown at the Fig. 2.7. As we can see, the area is a series of coordinates points that define the closed polygon. A part from selecting which is the first track to be flown, we can select the scanning azimuth angle, the separation between scanning traces, the entry and exit sides and the exit azimuth angle (thus all the possible scanning ways are taken into account). Thereby, once the user has introduced all that, as well as the departure airport an several more inputs, a sequence of legs are calculated automatically and translated into waypoints, thus describing the whole mission.

The scanning path, as we can see in the Fig. 2.6, is based on a series of parallel tracks, relative to an azimuth angle (±180º), that cover the whole area. The user is able to assign the entry point of the scan and which is the azimuth angle that he wants to has when leaving the scan. This pattern of parallel tracks is optimal for that sort of polygonal areas (when a goal of maximum scanning area is wanted) because it makes a sweep of the whole area leaving no blind zones and in a uniform way.

There are already implemented 4 sort of different legs regarding its use: Airfield, Basic, Control and Parametric Scan. The Airfield ones are related with operations to get to the airport or depart from it (due to its independence from

the rest of the operation) such as take-off, landing, taxiway path, etc. The Basic ones, including some RNAV leg types and extensions of them, such as Holding to a fix, Radius to fix, Track to fix, etc. The Control, which are control constructs that enable repetitive and conditional behavior. And the Parametric Scan ones, whose parameters will define the user needs (such as the area, Mach, altitude, entry/exit side of the area..) and will define the scan pattern.

It still lacks how a leg is defined. As we have said, the autopilot is fed with basic waypoints that allow the UA to perform a dynamical parametric scan over a RNAV-like flight plan manager, thus the whole procedure has to be defined by a sort of fly-over/fly-by/constant radius waypoints, its identifiers and coordinates[8]. Which is the same, the whole mission has to be determined by a sequence of Fix-to-Fix (Track-to-Fix or Direct-to-Fix) and Radius-to-Fix (RF) procedures. This way, there will be two different "traces": *arc* and *line*. So, all the different legs (holding to a fix, landing, turns, etc) will be ultimately defined by this two traces.

Regarding the turning maneuver, the Icarus UAS includes an enhanced extension of *Procedure turn to Intercept* (PI leg) track to be used as a turn maneuver. The PI leg is one of the 14 Area Navigation (RNAV) path-terminator legs defined in the Aeronautical Radio Inc (ARINC) 424 standard [16] and defines a course reversal starting at some specific point. Although PI legs are commonly used in approach procedures, it is extended so as to include it in the scan pattern. The reason of its using instead of a repeatedly RF turn is due to RF turns, although are the most efficient way to perform a turn, imply some limitations in the minimum track separation between scanning.

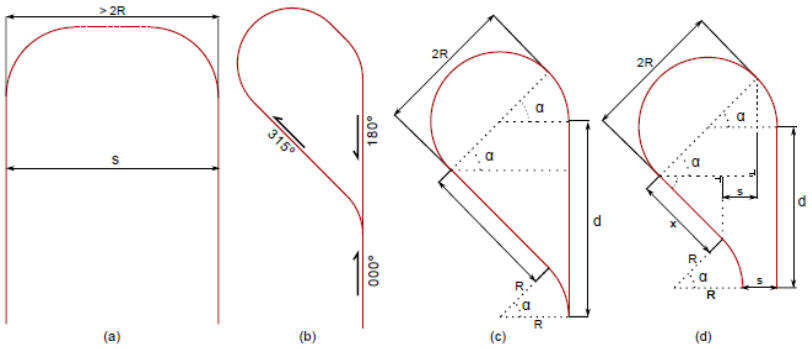

Fig. 2.8 Turn types implemented on the enviroment

In Fig. 2.8 we have the different kind of turns implemented as a function of s, the separation between two consecutive tracks. When $s \geq 2R$ (which depends on the bank angle and the airspeed) the turn path always follows a constant radius turn (RF) leg (case **a**). However, when $s < 2R$, two consecutive tracks

[8] A RNAV procedure is defined by: sequence of waypoints, path terminators included on ARINC 424, altitude and speed restrictions, direction of the turns and is required by navaids. Source: EUROCONTROL

cannot be linked by the previous way and an Enhanced Procedure to Intercept (ePI) leg is performed. The PI leg (case **b** and **c**) defines a course reversal starting at specific fix. The ePI (case **d**) is similar to the standard PI leg but the reversal track does not overlap the starting one. Instead, the reversal track is parallel to the one in PI leg but with a separation equal to s.

As it has been said, the whole system works because there exists an integrated sort of services that work together to accomplish that. Therefore, what is explained above is the basic implementations that the UAS needs in order to perform the dynamic parametrical mission, that is, a more complex architecture exists beyond all that.

That parameterizable scan pattern introduced is implemented within the ISIS simulation architecture [17]. ISIS is a service-oriented simulator that has been proposed to facilitate the investigation of several aspects of the introduction of UASs into non-segregated airspace, but also to test operational concepts related to the flight of UASs and their mission-oriented operation. ISIS employs multiple flight simulators (such as X-plane [18]) to realistically model the dynamic behavior of the selected UAS.

CHAPTER 2. Curved Scan Design

3.1 Parametric Design

Now that the theoretical aspects have been explained, both the context in which this kind of scans may be used and the environment in which that scans will be developed will be hypothesized.
We have seen how a Parametrical Scan it is already implemented and it is full optimal for scanning polygonal zones whose goal is not to have any "blank space" in the scan. However, in the context of a mission through an RFD[9] of a possible tornado, many tips may differ from the parameters of the previous scans:

-The desirable scanning area is no longer a polygon, but is a curved zone with two well defined boundaries

-The quickness in how the mission is done, is now much relevant, because depending on the storm behavior the needs may change

-The goal of the mission is not a scanning the whole area leaving no blind spaces, but crossing the RFD as many times and get data from the storm

-Due to the new requirements of the mission, a new turn implementation may be needed

-Many other possible applications for this new scan has to be taken into account for a parametrical generic solution

Thus, a new kind of scan has to be defined, a new algorithm developed and all that regarding the new parameters that define our new scan type. This new leg, the new scan type, will be named now one as Curved Scan leg, because the mission focuses on the fact that the zone is no longer a closed irregular polygon but a zone with curved shape.

3.1.1 Boundary interpretation

As it has been said, the scanning area will be defined with two boundaries. The user, probably the meteorologist in this case, will be in charge of selecting the set of points that will define both the North and South boundaries. One of the boundaries will be right set by looking at any of the meteo satellites due to RFD develop next to cold fronts or gust front (easily recognized on radars) and along to the development of the hook echo. However, the other can be placed in a "large" area due to two facts: the RFD area is quite big and when the RFD area

[9] As well as other atmospheric research.

finalizes it is not discrete. Therefore, the certainty that those points will exact correspond to the end/begin of the RFD area is more than doubtful. In addition, the storm is not static thing, so, the RFD will be displaced as well -not too much for short missions-, letting the boundaries being just a reference to sample the area.

What the user will really care is the UAS to fly fast and wisely through the RFD in a majority of the time of the mission, careless of the exactness of where the truly boundaries are placed in each moment. Because this, once the data will be collected, meteorologist may implement a mean measure or a discrimination algorithm of non useful data in order to get the thermodynamic data that they need of the RFD.

Due to these reasons, instead of interpolating the different boundary points in order to get a curve of a certain degree of fitting -which would be needed for a highly precise mission-, the boundaries have been defined as a sort of straight segments defined by the sort of points introduced by the user. This way, it will be obtained the Northern and the Southern boundaries. The boundaries will be differentiated by imposing that the Northern boundary must include the point with greatest latitude of the set of points of both boundaries. Thus, in order to get a closed area, between the two outer points of the each boundary, two straight "imaginary" lines will be created so as to get a closed polygon. These points, as well, will define the 4 possible Entry Points of the scan. An example of a possible scanning area would be the next:

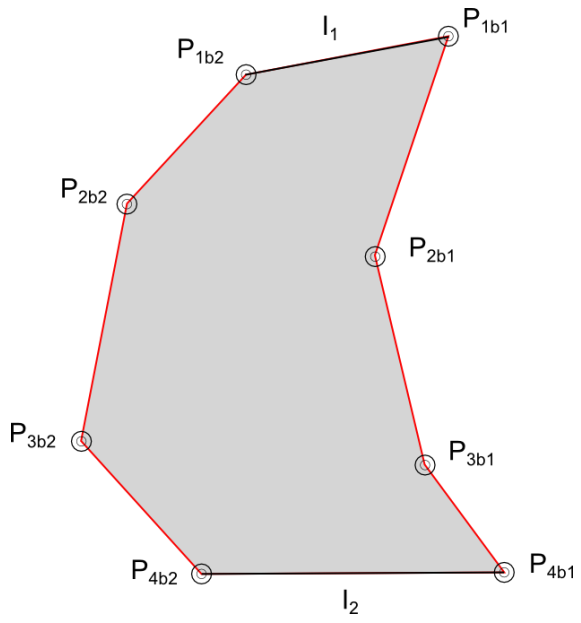

Fig. 3.1 Example of curved scan area, defined by two boundaries and their points

The user will be in charge of selecting a sort of points in order to define the segments that will define each boundary. In addition, between the outer points of each boundary two straight lines will be defined in order to establish what is

going to be the scanning area and, thus, its final shape. Finally, as we have said the possible entry points would be any of $P1b1, P4b1, P1b2$ and $P4b2$. In a generic way, and introducing the points in a sorted way, for any number of points introduced by the user, the entry point of the scan will be any of the firsts/last points of each boundary. About the exit point of the scan, it will be placed at any point of one of the two "imaginary" segments depending on the entry point -the further one-. Once the scan gets to this point, it will be over.

3.1.2 Geographical interpretations

As this is a geographic problem, the first thought was whether using a Cartesian coordinate system or using a Geodesic one. It is true that for small areas, like RFDs are, a Cartesian coordinate system like UTM projection, it will have suited perfect because it has a little error assuming a local flat earth. However, if we want to use this algorithm for other uses -see at Chapter 4-, this assumption imply a great error because of the Ellipsoidal shape of the earth now it is significant. Therefore, in order to take into account the possible other applications of this new type of scan, a geographic model of reference is used. Specifically, it has been used the projection WGS 84.

To do that, it has been needed to define a centre of the scanning area. At it has been said, we have considerate the scanning area as a closed polygon, thus, for irregular polygons, it is unlikely to have a point equally distanced from the vertex. Therefore, a centroid has been computed to define both a reference meridian and parallel. This way, each points of the boundaries has been defined using the WGS84 projection model.

The centroid of the polygon, $C = \{Cx, Cy\}$, is computed being $Pi = (X_i, Y_i)$, where $i = 1,2,3,..,N$ are the vertex of the area A.

$$Cx = \frac{1}{6A}\sum_{i=1}^{n-1}[(X_i + X_{i+1})(X_iY_{i+1} - Y_iX_{i+1})\,] \quad \textbf{(2.1)}$$

$$Cy = \frac{1}{6A}\sum_{i=1}^{n-1}[(Y_i + Y_{i+1})(X_iY_{i+1} - Y_iX_{i+1})\,] \quad \textbf{(2.2)}$$

where A is the area of the closed polygon, which is calculated

$$A = \frac{1}{2}\sum_{i=1}^{n-1}[(X_iY_{i+1})(X_{i+1}Y_i)\,] \quad \textbf{(2.3)}$$

3.1.3 Scanning angle interpretation

The first thought to develop the algorithm was to define the angle of scan as an angle relative to the normal line of the rebounded segment, that is, defining scanning angle dependant of the boundary shape. For example, given a random curved area, a scanning angle α and a entry point Ep:

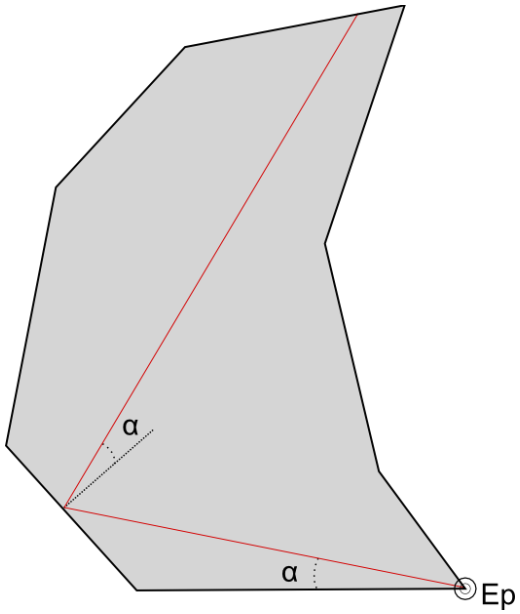

Fig. 3.2 Scan algorithm defining the angle α relative to the boundary shape

We can see that this particularly shape, and the fact of depending on the orientation of the segments, produce a premature leaving of the scan area and a non-efficient way to scan it. In addition, it may happen that any particular boundary shape would lead to a non-convergence pattern. Therefore, defining the angle this way seemed to be wrong due to the highly dependency on the inter-orientation of the boundaries, making the algorithm little robust for a general application.

Thus, another way to allow the user to have a design control parameter of the scan needed to be found, keeping in mind the idea of sampling the area by using a kind of angle selected by the him.

The idea has been to find a way to define the user angle, keeping independent how the segments of the boundary are orientated between each other, and taking into account the optimal orientation that the scan should has. Regarding the fact that each pair of points of each boundary defines a mean vector, $\overrightarrow{V_1}$ and

$\overrightarrow{V_2}$, a scan Vector of Reference ($\overrightarrow{Vref}$) has been defined[10], unique for each area and shape, that will be the arithmetic mean of the mean vector of each boundary. It is obvious that $\overrightarrow{Vref}$ will depend on how the course of the algorithm is.

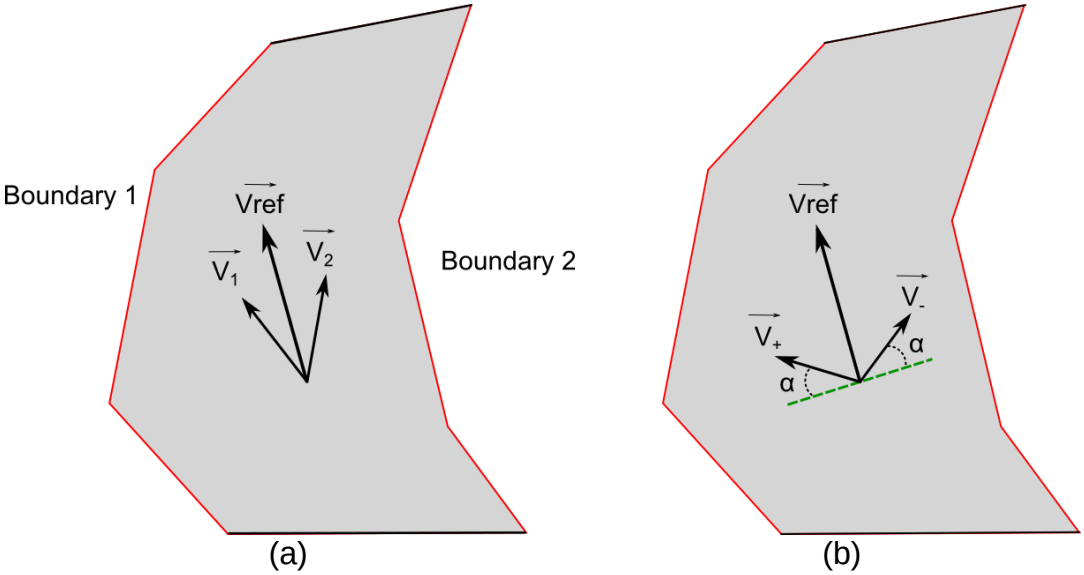

Fig. 3.3 Vector of Reference (a): defining the Vector of Reference as the mean vector of the mean vectors of each boundary (b): rotation of the Vector of Reference depending the α degrees selected by the user

As we can see in the Fig. 3.3, letting the points given by the user on the left side be the Boundary 1 and the ones on the right Boundary 2, the mean vectors $\overrightarrow{V_1}$ and $\overrightarrow{V_2}$ have been computed. They are extrapolated from the vectors that form each pair of points of each boundary. So, given these two vectors, $\overrightarrow{Vref}$ has been computed as the arithmetic mean of $\overrightarrow{V_1}$ and $\overrightarrow{V_2}$. Then, as it is shown in the Fig. 3.3 (b), rotating $\overrightarrow{Vref}$ $\pm(\frac{\pi}{2}-\alpha)$ degrees, we obtain both $\overrightarrow{V_+}$ and $\overrightarrow{V_-}$. Finally, this two vectors will define how the traces of the scan pattern will be, on one sense and into the other. They will be independent of the segments inter-orientation but the whole scan will proceed in an optimal orientation, thus always converging.

For example, for the area that is being used and a possible entry point Ep and a random scanning angle -selected by the user- α, we would obtain the following traces:

[10] ±180º depending on the entry position, that will determine the scan's orientation

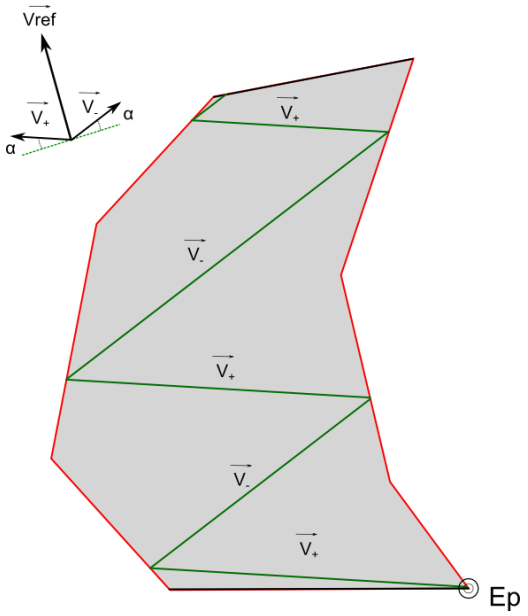

Fig. 3.4 Example of the scan algorithm

The way $\overrightarrow{Vref}$ is defined, dependent of the boundaries shape and the entry position of the scan, implies that as α rises, the way the scan is going to be flown will be faster as well. And, in a logical way, as α decreases, more traces will be performed in the operation, and thus, the time will rise too.

Finally, we note that the range of α is $\epsilon\{0,180\}$ degrees regarding that once α is greater than 90º, $\overrightarrow{V_+}$ and $\overrightarrow{V_-}$ exchange. It cannot be negative because, otherwise, the direction of the scan would be opposite from the desirable.

3.1.4 Refinement of the algorithm

If we take a look on the Fig. 3.4, what we can easily see is that the first trace that initiates at the entry point is not optimal because it covers a small area. Due to the way how $\overrightarrow{Vref}$ is obtained and defined, depending on the interposition of the outer points of each boundary, in this firsts steps, a suboptimal solution may be found. The solution has been to mix the first non optimal explained algorithm with this one.

For only once, the first trace will be flown following the same angle α defined by the user but now relative to the alongside imaginary line that exists between the entry point and the closer outer point of the other boundary. The result will be a first dependence of the interposition of the points of the two boundaries, thus giving a chance to explore zones where, depending on the outer points position, otherwise, following the previous algorithm, would not be scanned. From then on, the algorithm will keep being the same, using the traces given by the previous $\overrightarrow{V_+}$ and $\overrightarrow{V_-}$.

As we can see in the next Fig. 3.5 (a), for this another shape, with entry point Ep and selected angle α, the need for a refinement of the algorithm is well shown, as the bottom right part of the area is simply skipped. In the Fig. 3.5 (b), we can see that by first scanning with α degrees respect to the closer imaginary line and then keep on with the algorithm, using $\overrightarrow{V_+}$ and $\overrightarrow{V_-}$. traces, the scan covers all the area that was previously left off it. Note that now, the algorithm allow the scan to rebound in the closer imaginary for a better scan pattern.

Finally, it might happen that the user would use a too great α. In the shown entry point, it is not a problem but, if the entry point was the one on the top left corner, it could be a problem. This way, if the user wants to select a high α, if that let to any rebound, the algorithm looks for the maximum α that possibilities a rebound on the opposite boundary, given the entry point and the boundary geometrical characteristics. This way, once the rebound exists, this new angle will be forgotten and, as it has been explained, $\overrightarrow{V_+}$ and $\overrightarrow{V_-}$ will define the scan then on.

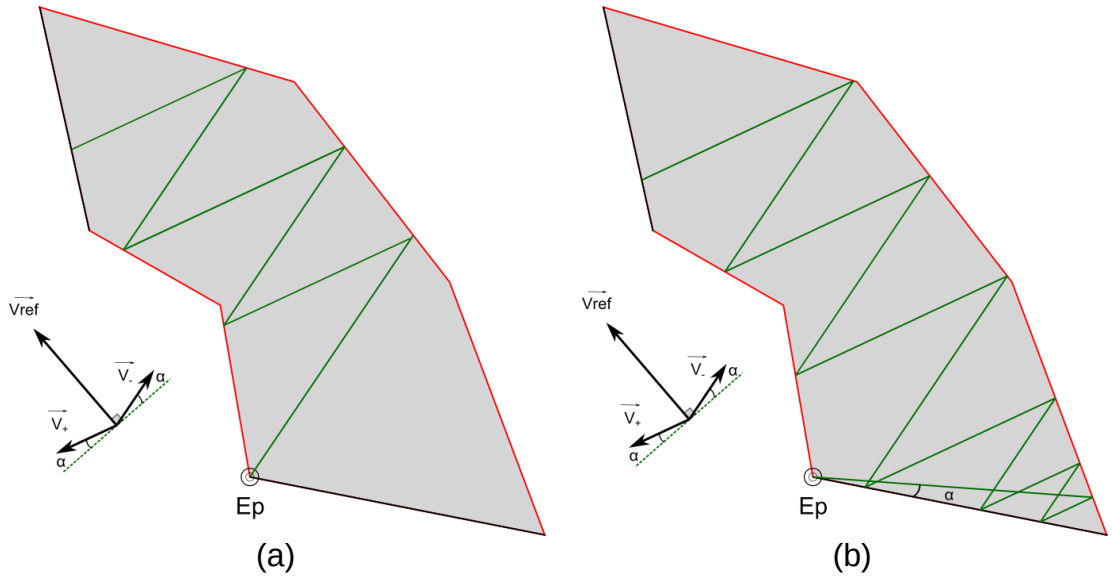

Fig. 3.5 Improvement of the algorithm (a): general view of a suboptimal scan operation for an entry point Ep and a scan angle (b) refinement of the first step of the algorithm so as to take into account interposition of the boundaries

However, regarding this last picture we realize a need for a new refinement in the last steps of the scan pattern, in the top left of the area. Again, a part of the scan area is omitted, but now, in the final part of the scan. What it would be worth is to, rebound against the other imaginary line, likely it is done in the first steps, so as to cover a greater part of the area. So, the resultant algorithm, once this improvement has been applied, will look like this:

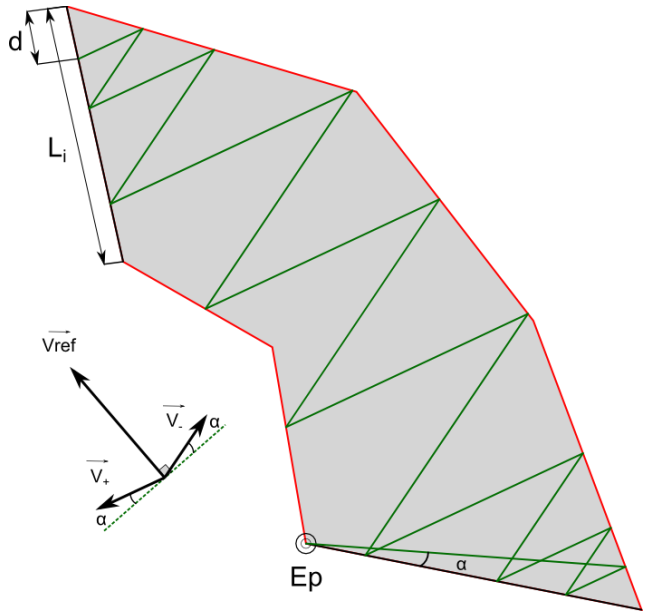

Fig. 3.6 Refinement of the lasts steps of the algorithm

The scan pattern will be as shown in Fig. 3.6. On the final steps, the scan pattern will be rebounding against the imaginary line (of length L_i) until the distance remaining to get to the end of the area, d, is $d < \frac{L_i}{4}$, this way finishing the scan pattern. This distance is a control parameter that is a trade-off between how much area -thus the number of samples- do you want to cover and how fast do you want to fly over it. A low d would imply a pretty inefficient solution for a quick mission as overfly RFD is, because more samples will be done. However, a great one would imply ignoring a significant area making the scan being even faster and, as before, depending on the goal of the missions, it may cannot be allowed.

3.2 Turn description

Once we get to this point, the only issue that remains to be explained is how the traces are flown. Specifically, how one trace is connected with the next. It is obvious that a turn like that, staring at the previous examples, -with no maneuver added- those turns cannot be flown by a UA. Therefore, it is needed to add some traces, again based on Fix-to-Fix and Radius-to-Fix procedures, so as the aircraft to be able to connect one trace with the consecutive one.

3.2.1 Standard Simple Turn leg

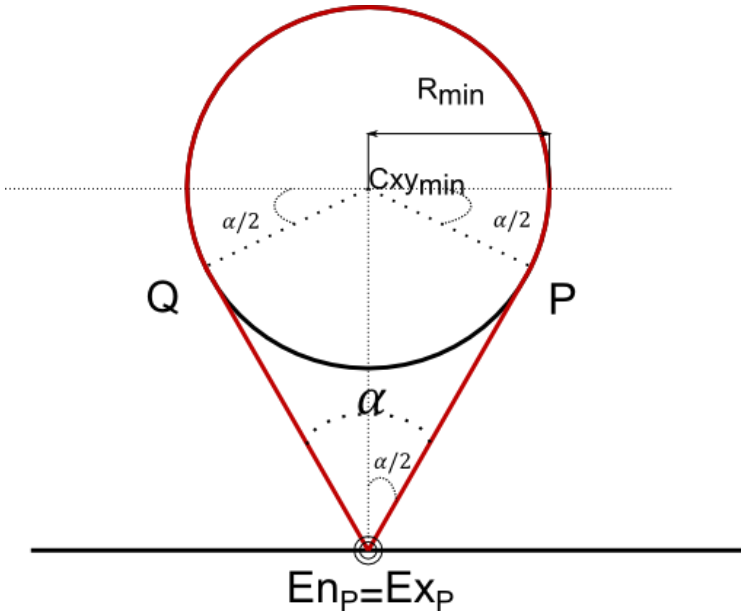

Fig. 3.7 Standard Simple Turn Leg overview

So, the proposed path for the UA to follow in order to intercept the right course and the next trace is the one in Fig. 3.7. To begin with, as the entry point of each turn is known because is the intersection between the actual trace and the boundary, we will assume this point as the a reference. Note that the black straight line is not any boundary, it is displayed with geometric reasons. In this case, we have to delimit the problem by using the constrain that the entry point of the turn En_p -the point where the plane leaves the scan area with a certain heading- must be the same as the last point of the turn Ex_p -when the plane comes back to the scan with another heading-.

First of all, we must found which is the minimum value of R: the minimum radius of turn that the plane can achieve. That would be implemented solving the next equation system 2.4 that came from the generic banked turn.

$$\begin{cases} L_y = \cos\beta \cdot L = mg \\ L_x = \sin\beta \cdot L = \dfrac{mv^2}{R} \end{cases} \quad \textbf{(2.4)}$$

$$\frac{\cos\beta}{\sin\beta} = \frac{g \cdot R}{v^2} \quad \textbf{(2.5)}$$

$$R_{min} = \frac{v^2}{\tan\beta \cdot g} \quad \textbf{(2.6)}$$

As we already know, the turn only depends on the speed and the bank angle of the plane. However, this time we have named it as R_{min} for a reason that will be explained before. We first need to define which is the height of the radius. That is, determine the y_{min} coordinate to place the center of the turn Cxy_{min}.

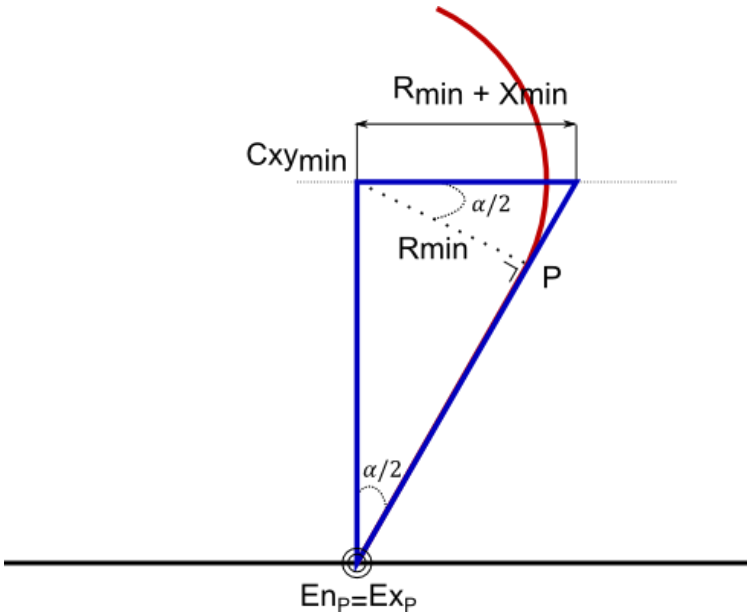

Fig. 3.8 Computation of the coordinates of the turn centre

First of all, as the first segment (the straight line with $\alpha/2$ degrees respect to y_{min} line) is perpendicular to the R_{min} dashed line at the P point, we can assure for trigonometric reasons that the angle between the R_{min} line at P and $R_{min} + X_{min}$ will also be $\alpha/2$ for any value of α from 0 to 90º.

In order to do that, we first have to look at the inner triangle (dashed line) from Fig. 3.8 so as to determine X_{min}.

$$\cos\frac{\alpha}{2} = \frac{R_{min}}{R_{min} + X_{min}} \quad \textbf{(2.7)}$$

$$X_{min} = R_{min} \cdot \left(\frac{1}{\cos\frac{\alpha}{2}} - 1\right) \quad \textbf{(2.8)}$$

And now that we know X_{min}, looking at the outer one from the Fig. 3.8 we can determine y_{min} and, thus, Cxy_{min} and the center of the turn.

$$\tan\frac{\alpha}{2} = \frac{R_{min} + X_{min}}{y_{min}} \quad \textbf{(2.9)}$$

$$y_{min} = \frac{R_{min} + X_{min}}{\tan\frac{\alpha}{2}} \quad \textbf{(2.10)}$$

So, now that we have the coordinates of the center of the turn $Cxy_{min} = (0, y_{min})$, we can derive Q and P points looking at the next triangle on Fig. 3.9. Note that Cx is 0 due to we have fix it with the constrains of the geometric problem.

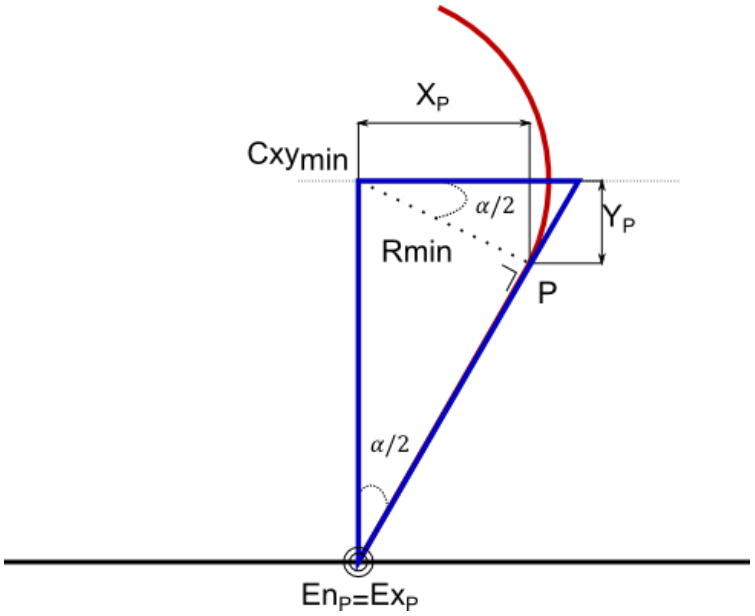

Fig. 3.9 Computation of the coordinates of the P point

$$x_P = \cos\frac{\alpha}{2} \cdot R_{min} \quad \textbf{(2.11)}$$

$$y_P = \sin\frac{\alpha}{2} \cdot R_{min} \quad \textbf{(2.12)}$$

So the coordinates of the P point will be $P = (Cx + x_P, Cy - y_P)$, which is equal to $P = (\cos\frac{\alpha}{2} \cdot R_{min}, Cy_{min} - \sin\frac{\alpha}{2} \cdot R_{min})$. Finally, as Q is a reflected point, we can define:

$$x_Q = \cos\frac{\alpha}{2} \cdot R_{min} = -x_P \quad \textbf{(2.13)}$$

$$y_Q = \sin\frac{\alpha}{2} \cdot R_{min} = y_P \quad \textbf{(2.14)}$$

And this way, $Q = \left(Cx - x_Q, Cy - y_Q\right) = (-\cos\frac{\alpha}{2} \cdot R_{min}, Cy_{min} - \sin\frac{\alpha}{2} \cdot R_{min})$. Thus, all the procedure it is defined by a set of waypoints based on fix to fix and radius to fix procedures and the goal that we wanted to achieve is accomplished.

3.2.2 Extended Simple Turn leg

For example, depending on the kind of scan that it is being done, it could be interesting to scan a zone while doing the turn, and it may happen that this zone is further from the center of the previous turn Cxy_{min}. In addition, I may happen that we must leave the zone of the scan for a certain time so, it would be worth to extend the turn maneuver until the UAV could come back to carry on with the scan. That is, the new y would be expressed as $y_{new} = y_{min} + \Delta y$ and the new Cxy will be Cxy_{new}.

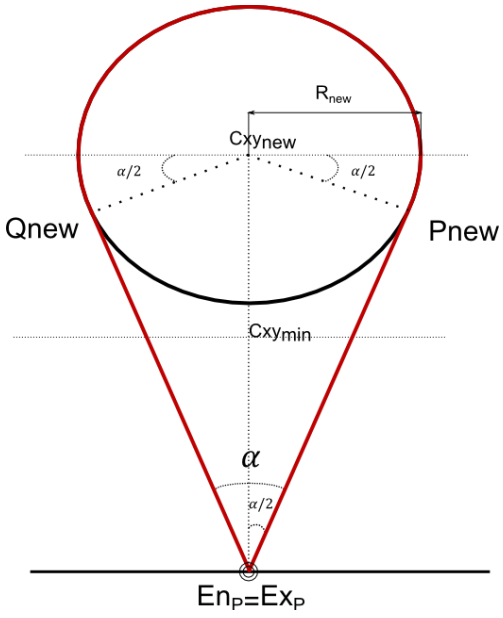

Fig. 3.10 Simple turn with and extended y coordinate point

However, in case that this Δy was too big, this turn may be too large. So, even we might want to fly this way, we may want to do a shorter turn procedure. There will be a way to do it, reducing the radius-to-fix part distance, by using 2 turns of radius R_{min} and keeping the same previous intersection points $P_{new}$and Q_{new} as well as the entry/exit point and α. The only drawback it would be that now, the turn will not be centered at Cxy_{new} but at some point below it.

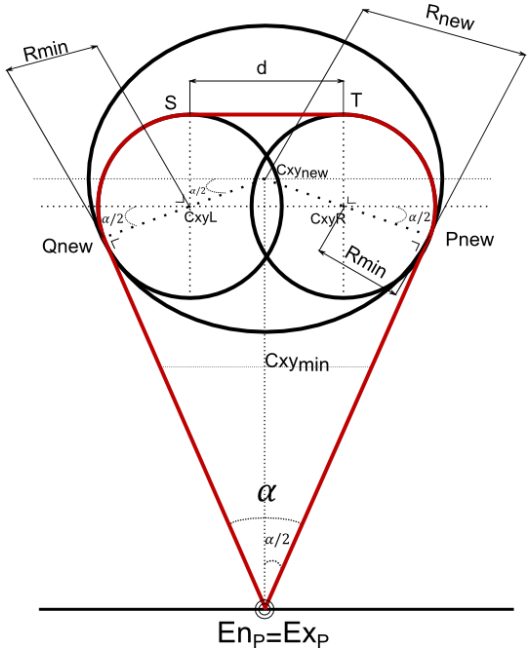

Fig. 3.11 Extended Simple Turn leg

The maneuver will proceed as follows: the UAS will fly at his previous heading (probably $\overrightarrow{V_+}$ or $\overrightarrow{V_-}$). until intersects the P_{new} point. Then, it will fly a radius-to-fix for $\frac{\alpha}{2} + 90$ degree respect to $CxyR$ or $CxyL$ that will have R_{min} of radius and, regarding all the restrictions we have imposed, it will be placed at some point at R_{new} line. When that it is over, the plane will fly straight for a distance d, and will fly again a radius-to-fix turn for $\frac{\alpha}{2} + 90$ degree, but now respect to the other $CxyR$ or $CxyL$ that, again, will have R_{min} of radius. This way, Q_{new} point will be intersected and the UAS will then be flying at the desired exit heading (again, probably $\overrightarrow{V_+}$ or $\overrightarrow{V_-}$) .

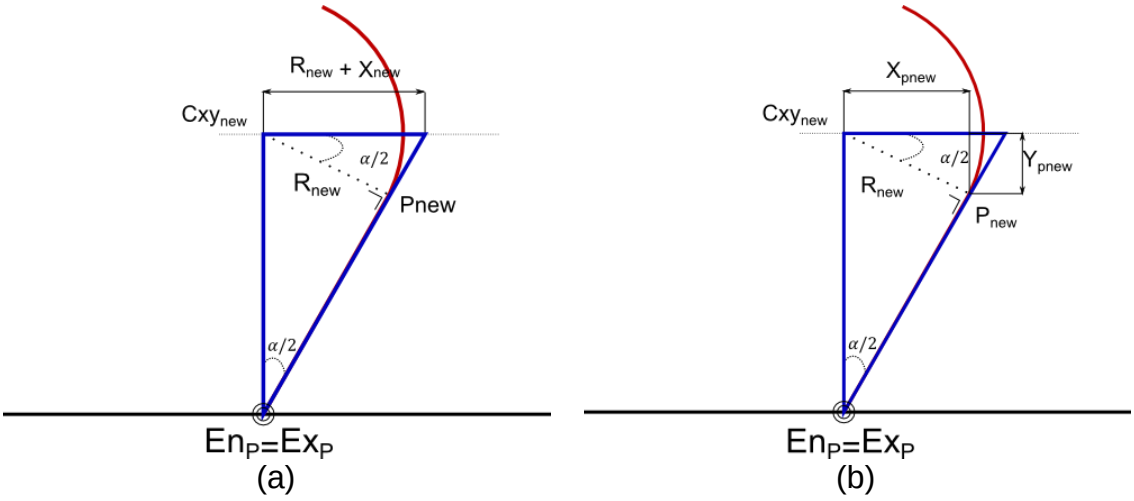

Fig. 3.12 Extended Simple turn computations (a): Computation of Rnew distance (b): Computation of Pnew coordinates

At Fig. 3.12 (a), from the inner dashed and outer blue triangles we obtain the next two relationships,

$$\tan\frac{\alpha}{2} = \frac{R_{new} + X_{new}}{y_{new}} \quad \textbf{(2.15)}$$

$$\cos\frac{\alpha}{2} = \frac{R_{new}}{R_{new} + X_{new}} \quad \textbf{(2.16)}$$

Now, isolating X_{new} and replacing it in the first equation we can derive R_{new}

$$X_{new} = R_{new} \cdot \left(\frac{1}{\cos\frac{\alpha}{2}} - 1\right) \quad \textbf{(2.17)}$$

$$\tan\frac{\alpha}{2} \cdot y_{new} = R_{new} \cdot \frac{1}{\cos\frac{\alpha}{2}} \quad \textbf{(2.18)}$$

$$R_{new} = \sin\frac{\alpha}{2} \cdot y_{new} \quad \textbf{(2.19)}$$

So, again, the coordinates of P will be $P_{new} = \left(Cx_{new} + x_{P_{new}}, Cy_{new} - y_{P_{new}}\right) = (\cos\frac{\alpha}{2} \cdot R_{new}, Cy_{new} - \sin\frac{\alpha}{2} \cdot R_{new})$ and Q, as it is just the reflected point, $Q_{new} = \left(Cx_{new} - x_{Q_{new}}, Cy_{new} - y_{Q_{new}}\right) = (-\cos\frac{\alpha}{2} \cdot R_{new}, Cy_{new} - \sin\frac{\alpha}{2} \cdot R_{new})$. What it is needed to define is $Cxy_{left}, Cxy_{right}, T, S$ and d. Cx_L and Cx_R are easily computed regarding both the triangles that their components form respect to R_{min} and the triangles that Cxy_{new} and its components form respect to R_{new} at the Q_{new} and P_{new} points.

$$Cx_R = \cos\frac{\alpha}{2} \cdot \mathrm{R_{new}} - \cos\frac{\alpha}{2} \cdot \mathrm{R_{min}} = \cos\frac{\alpha}{2} \cdot (R_{new} - R_{min}) = -Cx_L \quad \textbf{(2.20)}$$

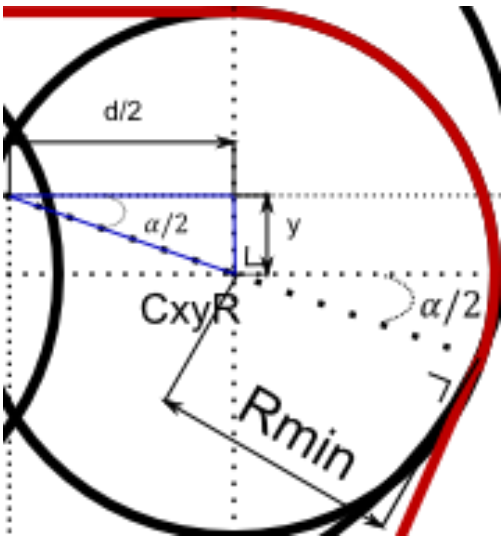

Fig. 3.13 Computation of d distance

As we can see at Fig. 3.13, the addition of the two components of $CxyR$ or $CxyL$ on the X axis is d, $d = Cx_R + |Cx_L| = 2 \cdot \cos\frac{\alpha}{2} \cdot (R_{new} - R_{min})$. So, what it lacks to be found out are Cy_L and Cy_R as well as define S and T points.

Regarding the previous triangle we can easily derive the Y component,

$$y = \tan\frac{\alpha}{2} \cdot \frac{d}{2} \quad \textbf{(2.21)}$$

$$Cxy_R = \left(Cx_{new} + \frac{d}{2}, Cy_{new} - y\right) = \left(\frac{d}{2}, Cy_{new} - y\right) \quad \textbf{(2.22)}$$

$$Cxy_L = \left(Cx_{new} - \frac{d}{2}, Cy_{new} - y\right) = \left(-\frac{d}{2}, Cy_{new} - y\right) \quad \textbf{(2.23)}$$

And, finally, $S = (\frac{d}{2}, Cy_{new} + R_{min})$ and , $T = (-\frac{d}{2}, Cy_{new} + R_{min})$. This way, again, all the procedure is defined as we wanted. To finish up with this task, it has to be said that for any $\Delta y > 0$ performing this last kind of turn would save both time and fuel because the distance flown it will be always smaller than just flying with R_{new} radius-to-fix procedure. That can easily be demonstrated just by integrating both areas under their defined curves. As, applying the restrictions, R_{new} will be always higher than R_{min} and the integral will always be smaller for that last case. Then, it will be a user task to appropriately select the interesting turn for him.

3.3 Implementation of the algorithm inside the environment

Finally, all this have to be implemented inside the simulator.

As it has been explained in the chapter 2.3, the environment is divided in 4 different legs; Airfield, Basic, Control and Parametric Scan legs. In order to develop the algorithm explained in the previous chapters, as well as the implementation of a new turn type, several classes and its related generators have been created.

In the Basic leg type, the class STLeg (Simple Turn) has been created. It is already explained how this turn is defined, but mainly, the class is defined by a direction -left or right turn- and two headings -the one that has at the entry point and the one that has to have in the exit point-. In addition, some other classes has been modified so as to understand new definitions for this turn.

In the Parametric leg type, the class Curved Scan has been created, implementing the algorithm explained in 3.1. In it, the basic properties to define this new scan are established. The Fig. 3.10 shows the eXtensible Markup Language (XML) parameter description of the proposed scan.

```
<leg id="MissionLeg" xsi:type="fp:CurvedScan">
                        <angle>20</angle>
                        <entryoffset>10</entryoffset>
                        <exitoffset>10</exitoffset>
                        <speed>150</speed>
                        <altitude>4500</altitude>
                        <NorthBoundary>
                                <point>42.774603 1.006161</point>
                                <point>42.739914 1.160689</point>
                                <point>42.644275 1.255575</point>
                                <point>42.523294 1.299903</point>
<!-- More points may follow -->
                        </NorthBoundary>
                        <SouthBoundary>
                                <point>42.675936 1.034753</point>
```

```
                                    <point>42.639586 1.10285</point>
                                    <point>42.570503 1.116767</point>
<!-- More points may follow -->
                                </SouthBoundary>
                                <ExitOrientation>True</ExitOrientation>
                                <VerticalEntryPoint>false</VerticalEntryPoint>
                                <HorizontalEntryPoint>false</HorizontalEntryPoint>
                                <iniTrack>1</iniTrack>
                            </leg>
```

Fig. 3.14 Example of a basic XML structure for parametric Curved Scan

Speed and altitude, the basic attributes, are the ones at which the scan operation should be carried out, measured in knots and feets respectively.

The specific ones for this scan type are the next:

- **angle:** In decimal degrees, will define the optimal trace's heading, $\overrightarrow{V_+}$ and $\overrightarrow{V_-}$, of the scan.
- **entryoffset:** Additional offset added at the beginning of the first track to compensate for any potential between the new leg and the previous.
- **exitoffset:** Additional offset added at the end of the last track to compensate for any potential misalignment between the new leg and the previous.
- **NorthBoundary:** The set of points, as a pairs of latitude / longitude WGS 1984 coordinates (in decimal degrees), that defines one of the boundaries of the area to scan. That set of points must contain the point with the greatest latitude.
- **SouthBoundary:** The set of points, as a pairs of latitude / longitude WGS 1984 coordinates (in decimal degrees), that defines the other boundary of the area to scan.
- **ExitOrientation:** Boolean value. Define the orientation of the last leg of the scan. A *true* value would imply that the last leg will be $\overrightarrow{V_+}$ and a *false* one would imply that it will be $\overrightarrow{V_-}$. If the last leg doesn't correspond to the desired one, that is removed to fulfill with this requirement -due to the main traces of the scan are $\overrightarrow{V_+}$ and $\overrightarrow{V_-}$, this is always true-. This way a sense of quickness for the mission is achieved too.
- **VeritcalEntryPoint:** Boolean value. Between the 4 possible entry points -the first / last points of each boundary-, a *true* value would imply selecting the two points with greater latitude. A *false* value would imply selecting the two points with lower latitude.
- **HorizontalEntryPoint:** Boolean value. From the selected points with the VerticalEntryPoint value, a *true* value would imply selecting the eastern one. A *false* value would imply selecting the western instead.

- **iniTrack:** Once all of the scan tracks have been defined according to the previous parameters, the iniTrack tag identifies the first track to be flown -skipping the rest-.

This way, the user will select two sets of points. The set with the greatest latitude point will correspond to the Northern boundary and the other to the Southern. From that point, two possible $\overrightarrow{Vref}$ (±180º) could be obtained. Then, by first selecting whether you want to entry into the scan from the northern or from the southern points (VerticalEntryPoint), and then choosing between the point at the east or at the west (HorizontalEntryPoint), the correct orientation for $\overrightarrow{Vref}$ is selected. So, once the user select the desired angle, possible incompatibilities are computed and so is the first trace, to avoid geometry irregularity problems. Then the main traces $\overrightarrow{V_+}$ and $\overrightarrow{V_-}$ are computed, and so is the algorithm. Finally, depending on the orientation desired for the user for the last leg, selecting the ExitOrientation variable, this one may or may not be skipped, thus finalizing the whole mission.

CHAPTER 3. RESULTS

In this chapter, some examples of how the Curved Scan algorithm developed works will be shown. There also be shown how the user can change the control variables, the parameters of the scan, so as to fit at their needs, and how they change the scan pattern.

The next pictures come from a whole simulated mission done over the Pyrenees, departing from LERS, with all the legs needed, turn procedures for departing and landing, holdings, etc. The area to scan is the one used to describe the whole algorithm in previous sections.

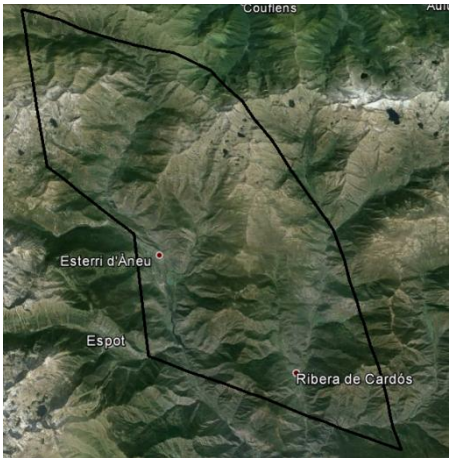

Fig. 4.1 Scanning area

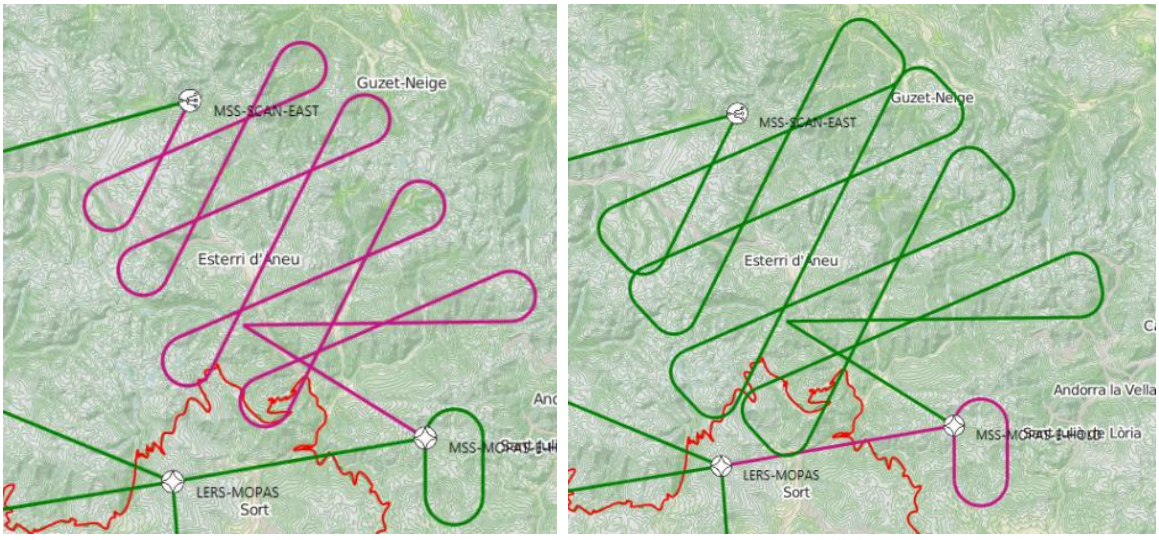

(a) (b)

Fig. 4.2 Curved Scan mission; 20º, Vertical = false, Horizontal = false, ExitOrientation = false. (a): Standard Simple Turn leg (b): Extended Simple Turn leg

In the Fig. 4.2 we can see how, for the same mission -in a parametrical point of view- the difference between the Standard and Extended Simple Turn leg.

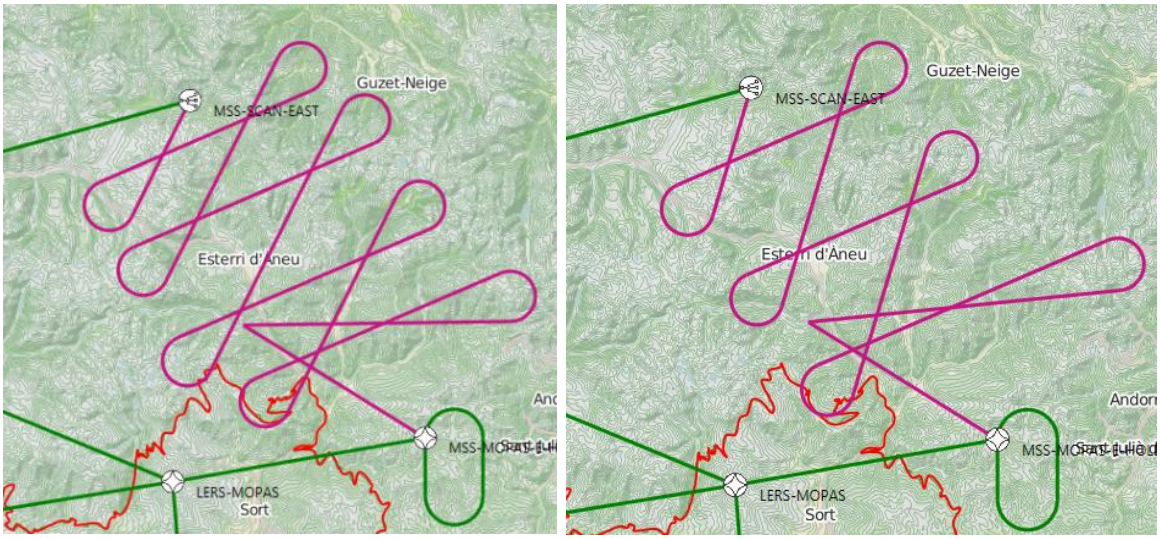

(a) (b)

Fig. 4.3 Curved Scan mission; Vertical = false, Horizontal = false, ExitOrientation = false (a): 20º (b): 25º

In the Fig. 4.3 how, for the same mission, changing the angle α allow the UA to perform less samples and a faster mission.

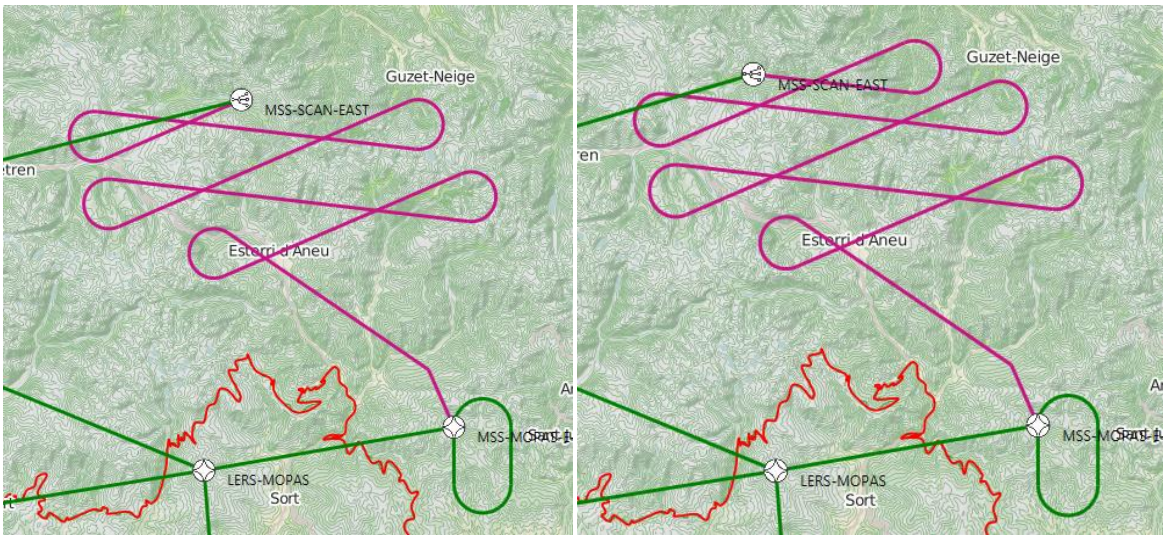

(a) (b)

Fig. 4.4 Curved Scan mission; 15º, Vertical = false, Horizontal = true (a):ExitOrientation = false (b): ExitOrientation = true

In Fig. 4.4 we see how the scan looks like when the entry point changes. Due to the area characteristics, in the first trace, as the angle given by the user let to

no rebound to the south boundary, this has been reduced -as it has been explained at 3.1.4- allowing the scan to be possible. In addition, we can see how the parameter ExitOrientation makes a much better perform in the case (b) than in the (a). In the (a) case the orientation is almost the opposite than the desired (case b).

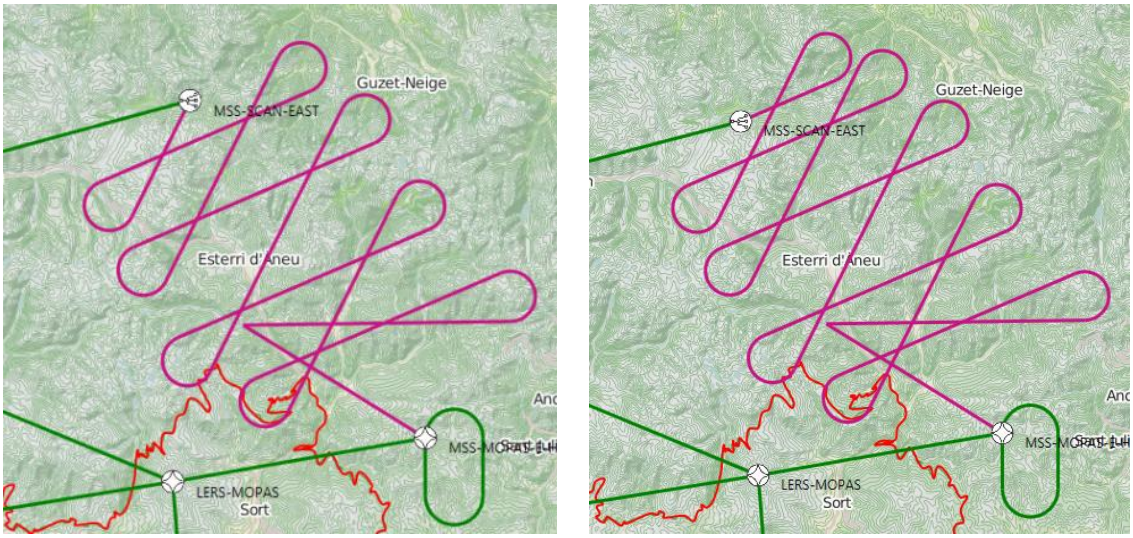

(a) (b)

Fig. 4.5 Curved Scan mission; 20º, Vertical = false, Horizontal = false, (a): ExitOrientation = false (b): ExitOrientation = true

Finally, in the Fig. 4.5 we see again the effects of changing the ExitOrientation, how the scan is much better when the orientation of the last scan is pointing to the next track.

CHAPTER 4. CONCLUSIONS

As it has been exposed, the propose of this study is to develop a generic algorithm for atmospheric research. In order to do such a task, firstly we have understand how the environment on the Icarus UAS is implemented works, specifically, how the already implemented Parametric Scan works. We have seen that the goals that this algorithm wants to achieve are quite different from the ones that the atmospheric research needs to fulfill.

This way, we have explained which the goals of this kind of missions would be so as to have in mind the target we wanted to achieve. We have named this new scan type as Curved Scan from the shape of the atmospheric phenomena. The algorithm of the scan has been developed following a discussion of how the physical phenomena can be approximated in a mathematical way. Then, we have explained how is the path of the scan that the UA had to follow and a refinement of this algorithm taking into account both the irregularities of the area desired to scan and the needs of this can of missions. We have also implemented two new turn types that fits to our algorithm, thus, finally, we have been able to develop a new scan type, in a parametric scan context, which is able to perform missions the way we desired, having as a base the hypothesis we made to describe this new kind of missions.

Indeed, the goal of this algorithm was to generate a scan pattern for a generic operation in atmospheric research. One of the constrains was, a part from the curved boundaries, a need for a quick mission, and that it was much more relevant to cross the desirable area as many times as it could than scanning the area leaving no blind spaces. This was mainly thought because in this kind of missions, the time constrain is important but as well as it is do as many samples as it can be done.

One of the main applications for this algorithm on atmospheric research, a part from the one in RFD, could be on the monitoring of volcanic plumes -ashes thrown away from inside of the volcano-. For civil aviation that is a capital issue due to its impact on both risking human life and for economical reasons (cancellations, insurances, engine damage, etc). For example, the economic impact of the volcanic ash from Eyjafjallajökull, in the aviation domain, is being estimated at €1.7 billion and a similar amount is thought to have been lost by the tourist service sector [19].

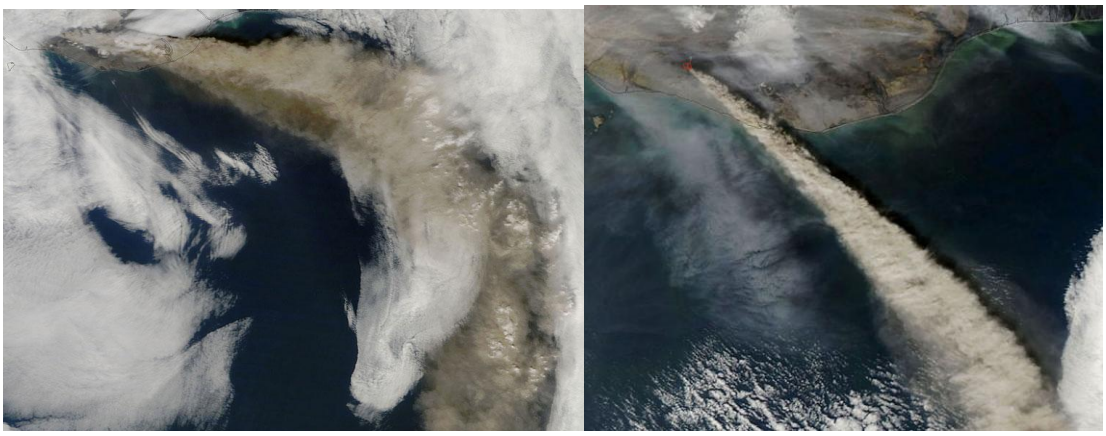

Fig. 5.1 Photograph of the volcano Eyjafjallajökull. By NASA/GSFC/Jeff Schmaltz/MODIS Land Rapid Response Team

So, estimating the ash density in $^{g}/_{m^2}$, as well as other properties inside the volcanic plumes, it then results so important because flights should not take off into airspace in which the actual ash density exceeds $2 \cdot 10^{-4} g/m^2$.

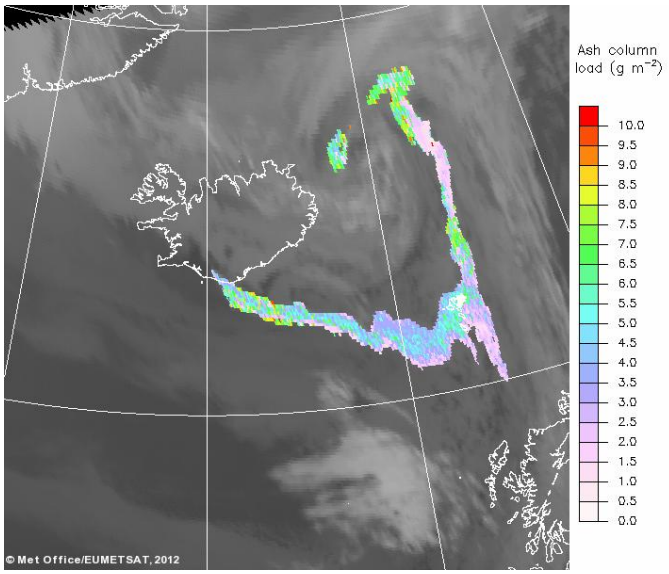

Fig. 5.2 Ash density of the volcano Eyjafjallajökull 2010

Therefore, as it is a clear Dull Dirty Dangerous (DDD) operation, the UAS platform suits perfectly because there exists no risk for human life that, otherwise, it would. We can easily see that, for this kind of operations, the Curved Scan developed matches. From the Fig. 5.1, and applying the algorithm of the scan, we can discern two curved boundaries and the traces that will be flown will make, depending on the angle selected by the user, a fast mission but with quite good amount of samples as well.

BIBLIOGRAPHY

[1] US GOVERNMENT, National Osceanic and Atmospheric Administration and National Weather Service, "Thunderstorms,Tornadoes, Lightning;Nature's Most Violent Storms," [Online]. Available: http://www.nws.noaa.gov/om/severeweather/resources/ttl6-10.pdf.

[2] A. B. Smith and R. W. Katz, "U.S. Billion-dollar Weather and Climate Disasters: Data Sources, Trends, Accuracy and Biases," 2014. [Online]. Available: http://www.ncdc.noaa.gov/billions/docs/smith-and-katz-2013.pdf. [Accessed 2014].

[3] National Climatic Data Center, "NOAA: Billion-Dollar Weather/Climate Disasters: Overview," 2013. [Online]. Available: http://www.ncdc.noaa.gov/billions/overview. [Accessed 2014].

[4] P. M. Markowski, "Hook Echoes and Rear-Flank Downdrafts: A Review," University Park, Pennsylvania, 2001.

[5] J. Elston, B. Argrow, E. Frew and A. Houston, "Evaluation of UAS Concepts of Operation for Severe Storm Penetration using Hardware-in-the-Loop Simulations," 2010. [Online].

[6] P. M. Markowski, J. M. Straka and E. N. Rasmussen, "Direct Surface Thermodynamic Observations within the Rear-Flank Downdrafts of Nontornadic and Tornadic Supercells," Norman, 2001.

[7] VORTEX2, "VORTEX 2 Project Summary," 2007.

[8] A. Houston, B. Argrow, J. Elston and J. Lahowetz, "Unmanned Aircraft Observations of Arimass Boundaries: The Collaborative Colorado-Nebraska Unmanned Aircraft System Experiment," 24th Conference on Severe Local Storms, 2008.

[9] NASA, "The Promise of ERAST," 2008. [Online]. Available: http://www.nasa.gov/centers/dryden/news/X-Press/stories/102904_people_erast.html.

[10] NASA, "Hurricane and Severe Storm Sentinel (HS3)," 10 2014. [Online]. Available: http://www.nasa.gov/mission_pages/hurricanes/missions/hs3/overview/index.html.

[11] NASA, "Genesis and Rapid Intensification Processes (GRIP)," [Online]. Available: http://www.nasa.gov/mission_pages/hurricanes/missions/grip/main/index.html.

[12] NASA, "Potential use of Unmanned Aircraft System (UAS) for NASA science misions," 2006. [Online]. Available: http://airbornescience.nasa.gov/program/documents.html. [Accessed 2015].

[13] E. Santamaria, E. Pastor, C. Barrado, X. Prats, P. Royo and M. Perez, "Flight Plan Specification and Management for Unmanned Aircraft Systems," *Journal of Intelligent & Robotic Systems,* Vols. doi:10.1007/s10846-011-9648-3, pp. 1-27.

[14] FAA, "Section 2. Area Navigation (RNAV) and Required Navigation Performance (RNP)," 2014. [Online]. Available: http://www.faa.gov/air_traffic/publications/atpubs/aim/aim0102.html. [Accessed 2015].

[15] P. Royo, M. Perez, R. Cuadrado and E. Pastor, "Enabling Dynamic Parametric Scans for UAS Remote Sensing Missions," Castelldefels School of Technology (EETAC), Castelldefels, 08860.

[16] ARINC, "ARINC SPECIFICATION 424-15," 2000.

[17] P. Royo, C. Barrado and E. Pastor, "ISIS+: A Software-in-the-Loop UAS Simulator for Non-Segregated Airspace," *Journal of Aerospace Computing, Information and Communication.*

[18] [Online]. Available: http://www.x-plane.com/desktop/home/.

[19] Dr. Thorgeir Pálsson, "Atlantic Conference on Eyjafjallajökull and Aviation," Keflavik Airport, Iceland, 2010.